plant biology

Plant Biology ISSN 1435-8603

RESEARCH ARTICLE

Searching new targets for the control of Black Rot: following the role of host factors modulating the infection process of *Phyllosticta ampelicida*

C. Tisch[1], A. Kortekamp[1] & P. Nick[2]

1 DLR Rheinpfalz State Education and Research Center of Viticulture and Horticulture and Rural Development, Neustadt an der Weinstraße, Germany

2 Molecular Cell Biology, Joseph Kölreuter Institute of Plant Sciences, Karlsruhe Institute of Technology, Karlsruhe, Germany

Keywords
Black Rot; European Wild Grapevine; *Phyllosticta ampelicida*; *Vitis sylvestris*.

Correspondence
P. Nick, Molecular Cell Biology, Joseph Kölreuter Institute of Plant Sciences, Karlsruhe Institute of Technology, Karlsruhe, Germany.
E-mail: peter.nick@kit.edu

Editor
H. Rennenberg

Received: 31 May 2023;
Accepted: 24 October 2023

doi:10.1111/plb.13598

ABSTRACT

- Black Rot is a grapevine disease caused by the ascomycete *Phyllosticta ampelicida*. Neglected so far, this is developing into a pertinent problem in organic viticulture as resistant varieties are still lacking. Here, we follow cellular details of the infection process in the susceptible *vinifera* variety Müller-Thurgau and screen the ancestral European wild grapevine (*V. vinifera sylvestris*) for resistance to Black Rot.
- Using a standardized infection assay, we follow fungal development using LTSEM and quantify key stages on different hosts using fluorescence microscopy.
- There is considerable variation in susceptibility, which is associated with more rapid leaf maturation. Hyphal growth on different carbon sources shows a preference for pectins over starch, cellulose or xylans. In the resistant *sylvestris* genotypes Ketsch 16 and Ketsch 18 we find that neither spore attachment nor appressorium formation, but hyphal elongation is significantly inhibited as compared to Müller-Thurgau. Moreover, defence-related oxidative burst and accumulation of phenolic compounds is stimulated in the resistant genotypes.
- We arrive at a model, where more rapid maturation of the cell wall in these *sylvestris* genotypes sequesters pectins as major food source and thus block hyphal elongation. This paves the way for introgression of genetic factors responsible for cell wall maturation into *V. vinifera* to develop Black Rot-resistant varieties of grapevine.

INTRODUCTION

The public debate on globalization is often biased towards purely economic processes. However, the concept has a much broader sense, namely as the process of integration and interaction of human activities (for a conceptual review see James & Steger 2014). Human mobility is, thus, at the core of globalization. There is, therefore, a strong impact of globalization on biology, for instance, because pathogens can move out from their centre of origin where they had co-evolved with their hosts and established a balance. Due to this migration, they often encounter related (domesticated) species that are naïve hosts, with devastating consequences (Taraschewski 2006). Viticulture can serve as a good example, because domesticated grapevine (*Vitis vinifera* L.) had to face, from the mid-19th century, several attacks of pathogens from North America, such as the aphid *Phylloxera* (now *Dactylosphaera vitifoliae* FITCH), the ascomycete *Erysiphe necator* (SCHWEIN.) BURRILL or the oomycete *Plasmopara viticola* (BERK. & M.A. CURTIS) BERL. & DE TONI. While the wild grapevine species in their region of origin had evolved resistance factors to contain these pathogens, the European grapevine was unprepared and, thus, an early victim of globalization (for review see Gessler *et al.* 2011). In consequence of climate change, such migrations become more frequent, and diseases that some years ago were still rare now have economic momentum.

One example for these newly emerging pathogens is *Phyllosticta ampelicida* (ENGELMANN) VAN DER AA (telomorph: *Guignardia bidwellii* (ELLIS) VIALA AND RAVAZ), a fungal pathogen causing Black Rot on grapevine. It is indigenous to North America but was introduced to Europe and also to South America, presumably on contaminated rootstocks used for their resistance to *Phylloxera* (Ramsdell & Milholland 1988). Also in North America, Black Rot can cause significant damage to *V. vinifera*, but also to commercially used hybrids with North American species (Gessler *et al.* 2006). In Europe, Black Rot was first reported around 1885 in France (Pezet & Jermini 1989), and has been limited to regions with moderate climate conditions such as southwest France (Jermini *et al.* 2009), northern Italy (Jermini *et al.* 2009), or southern Switzerland (Pezet & Jermini 1989). However, since 2002, Black Rot exerts increasing economic impacts in German wine-growing regions, especially in the northern wine growing areas, such as Mosel, Nahe and Middle Rhine, where weather conditions are favourable, and abandoned or overgrown vineyards serve as inoculum sources for this pathogen (Lipps & Harms 2004; Harms *et al.* 2005).

Black Rot has become an issue predominantly in organic viticulture, where synthetic fungicides cannot be applied, because products released for organic viticulture based on copper or sulphur do not currently provide satisfactory protection (Harms *et al.* 2005). However, in the northeast USA, it poses

major problems even in conventional viticulture. Although the degree of susceptibility to Black Rot differs among grape varieties to some extent (Loskill *et al.* 2010; Rex 2012), all commercially important cultivars are susceptible to this disease. However, certain genotypes of the European wild grapevine (*V. vinifera* subsp. *sylvestris*) have partial resistance to Black Rot, albeit the underlying mechanisms are not known (Schröder *et al.* 2015). Since current strategies of disease control are still far from optimal, knowledge of biology of the Black Rot pathogen and its infection process is essential to design more efficient strategies. This is especially true regarding the situation in organic viticulture.

Although there has been research on the cellular events of the infection cycle (Kuo & Hoch 1995, 1996a, b), for the economically relevant asexual cycle, numerous aspects remain open, especially with respect to energy supply during the initial biotrophic phase: from an epidemiological viewpoint, the asexually formed pycnidiospores are most relevant because they may generate repeated infections during a vegetation period. Pycnidiospores rapidly settle and adhere to the substrate after applying a droplet of spore suspension (Kuo & Hoch 1995), but they do not germinate before they have firmly attached to the surface (Kuo & Hoch 1996a). Attachment is supported by lipophilic surfaces such as the grape leaf cuticle, but also by water repellent artificial materials, such as polystyrene or Teflon (Kuo & Hoch 1996a). Immediately after attachment, most pycnidiospores germinate within 1 h. Subsequently, the tip of the germ tube swells and differentiates into an appressorium (Kuo & Hoch 1996b); subsequently, the cytoplasm moves into the appressorium and septa form (Shaw *et al.* 1998), leaving the empty pycnidiospore behind, which eventually collapses (Kuo & Hoch 1996b). Appressoria mature by incorporating melanin (Kuo & Hoch 1995), giving rise to their black colour. Emanating from the appressorium, a penetration peg breaches the cuticle and hyphae emerge, but remain limited to the subcuticular region (Kuo & Hoch 1996b). These hyphae expand and branch, developing a two-dimensional hyphal network above the anticlinal cell walls of the epidermal cell layer (Galet 1977; Kuo & Hoch 1996b; Ullrich *et al.* 2009), which is a characteristic feature of this pathogen (Kuo & Hoch 1996b). Additionally, short lateral branches grow on the periclinal wall of the epidermal pavement cells, but do not entirely reach across these cells (Kuo & Hoch 1996b; Ullrich *et al.* 2009).

The hyphal alignment was proposed to derive from lower resistance of the anticlinal cell wall (Kuo & Hoch 1996b). Alternatively, pectins, as main constituents of the middle lamella, were proposed to be more abundant in this zone (Kuo & Hoch 1996b), or apoplastic sugars and amino acids were suggested as spatial cues (Ullrich *et al.* 2009). Such speculations were related to the peculiar trait that *P. ampelicida* seems to lack haustoria, the typical feeding structures of other biotrophic fungi. Moreover, it does not penetrate the cell wall, nor directly kill the pavement cells. Thus, the mechanism of energy uptake during the relatively long biotrophic phase of this organism remains enigmatic. The situation resembles that in *Venturia inaequalis*, the causal agent of Apple Scab, which secretes pectin-degrading enzymes (Valsangiacomo & Gessler 1992; Kollar 1998).

To gain insight into the cellular aspects of pathogen–host interaction, and the potential mechanisms behind the partial resistance of certain *V. vinifera sylvestris* genotypes, we conducted a comparative study using controlled inoculation. For a prioritized set of genotypes with contrasting susceptibility, the asexual infection process of *P. ampelicida* was then followed using fluorescence microscopy and low-temperature scanning electron microscopy (FTSEM) imaging, extending the observation to later infection steps immediately before and during symptom expression, at the transition from bio- to necrotrophy, when pycnidia develop and mature for subsequent reproduction. Furthermore, to address the open issue of energy acquisition during the biotrophic phase, a plate assay was constructed to study the enzymatic potency of the pathogen in host-free conditions, and to define factors in the cell walls of the host that might act as targets for a future modulation or containment of the infection process.

MATERIAL AND METHODS

Plant material

For this study, a set of 82 genotypes of *V. vinifera* subsp. *vinifera* and subsp. *sylvestris* were investigated. Details on the accessions, including origin and voucher number are given in Table S1. All accessions are maintained as clonal vouchers in the germplasm collection of the Botanical Garden of the Karlsruhe Institute of Technology, Germany. Cuttings of the accessions were rooted and cultivated in the greenhouse in daylight and a mean temperature of 20 °C in 0.45-l pots filled with commercial substrate (Anzuchterde, Floragard, Oldenburg, Germany), supplemented with 5 $g \cdot l^{-1}$ coated fertilizer (15 N, 7 P, 15 K) (Manna, Düsseldorf, Germany) and 10 $g \cdot l^{-1}$ calcium carbonate (Kalkwerk Hufgard, Hösbach-Rottenberg, Germany) to buffer soil acidity. Plants were ready for experiments when they had reached a height of approximately 60 cm.

Propagation and inoculation of *P. Ampelicida*

Isolate '8088-2' of *P. ampelicida* originated from infected leaves exhibiting pycnidia of vines in an untreated vineyard in Kesten (Mosel) in 2005. The fungus was maintained on oatmeal agar (40 $g \cdot l^{-1}$ oatmeal, 20 $g \cdot l^{-1}$ agar) in Petri dishes at 25°C under continuous white light (L18-73 and L18W/840 Lumilux cool white; Osram, Munich, Germany). For weekly subcultivation, agar plugs (*ca.* 5-mm diameter) from actively growing mycelium (3–4 weeks on potato dextrose agar (PDA) at 21 °C in a 12 h/12 h light/dark cycle) were placed in the centre of fresh plates. To generate inocula for controlled infection of plants, fungal cultures that had produced pycnidia were collected 10–18 days after subcultivation by flooding the plates with 10 ml sterile distilled water. After 10 min, plates were rinsed, and pycnidiospore concentration adjusted to 25,000 spores·ml^{-1}. The early steps of infection were followed on leaf discs (Ø = 16 mm) collected from the fourth leaf below the shoot apex. Leaf discs were excised with a cork borer and transferred to Petri dishes (Ø = 90 mm) on moist filter paper soaked with 6 ml distilled water. Each leaf disc was inoculated with one droplet of inoculum (20 µl) and incubated for 24 h at 21 °C. After removing the remaining liquid with filter paper to avoid contamination by other fungi or bacteria, the Petri dishes were incubated in a plastic box covered with a transparent bag, to maintain high relative humidity, placed in a climate chamber at 21 °C and a day/night cycle of 12 h/12 h.

Quantification of infection *in planta*

To ensure standardized inoculation, entire plants were sprayed with a suspension of 25,000 conidia·ml^{-1} using a glass spray atomizer driven by pressurized air. The volume per individual plant was 15 ml. Following application, plants were kept at 100% humidity and 21 °C in the dark for 24 h because Black Rot requires long periods of high humidity for successful infection. Subsequently, plants were transferred to the greenhouse (40–50% humidity) and cultivated till analysis. We marked the plant tip immediately after inoculation with a fine thread, such that we could assign leaf positions at the time of symptom evaluation, 20 days post-infection (dpi) along the plant axis, starting from the infection site – leaves towards the base were counted as positive numbers, leaves towards the apex (newly formed during incubation) as negative numbers. Since infection of these leaves was presumably secondary, we used them only to assess developmental progression of susceptibility (Fig. 1B), but excluded them from the score, when monitoring overall susceptibility of a given genotype (Figure S3). We used two quantitative parameters: infection frequency determined as proportion of symptomatic leaves over the entire population of leaves. Thus, this parameter did not consider whether a given leaf was only weakly infected or entirely covered by mycelium. Therefore, we used infection severity as second quantitative readout. We scored infection based on relative coverage of leaves following the European Plant Protection Organization (EPPO) guideline PP1/4(4) for *Erysiphe necator* (EPPO 2020; Table 1). For both, we averaged the scores over leaves of the same condition from three different plants. Due to space limitations, we could only investigate 30 accessions in one experiment, such that the entire study required several infection campaigns. We verified the consistency of cultivation and infection conditions by including three individuals of the commercial variety *V. vinifera* cv. 'Müller-Thurgau' as internal standard in each experiment. Data for disease frequency and severity represent mean ± SE from three to 12 independent experiments with three individuals per experiment and genotype.

Molecular phylogeny based on whole genome sequencing

For a significant proportion of the *V. sylvestris* population (29 genotypes), whole genome sequences were available that had been established during a phylogenetic study on 472 accessions of *Vitis* including 64 *V. sylvestris*, but also 177 domesticated varieties of *V. vinifera* (Liang *et al.* 2019). Based on the entire set of Single Nucleotide Polymorphisms (SNPs) of these 472 genomes, a phylogenetic tree was inferred using the Maximum Likelihood strategy based on 100 bootstraps using the software SNPhylo58 (Lee *et al.* 2014).

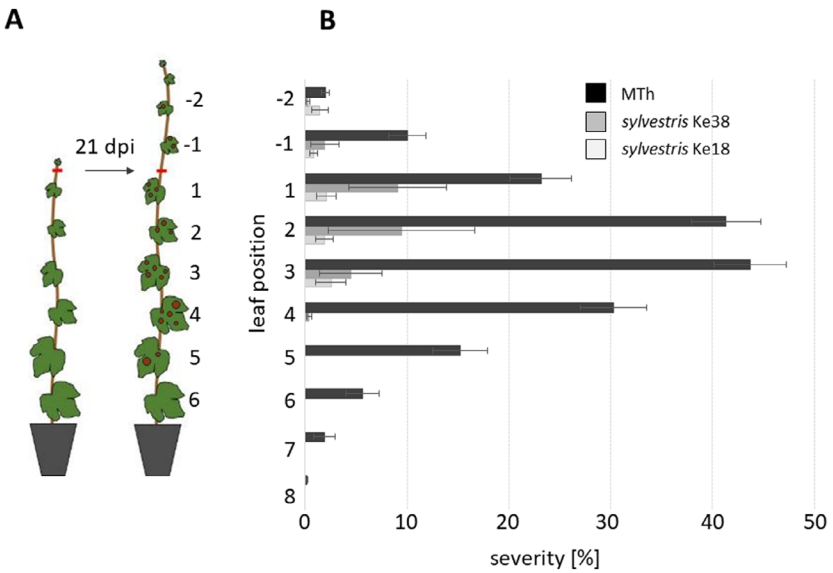

Fig. 1. Severity of Black Rot symptoms depends on genotype and leaf age. (A) Experimental design. Leaves are numbered from the apex at the time of inoculation (red line). Negative numbers indicate that the leaves have arisen newly during the 21 days post infection (dpi). (B) Disease severity at 21 dpi depending on leaf position for the economically important German vinifera variety Müller-Thurgau (MTh), and for two sylvestris genotypes from the last viable population on the Rhine peninsula Ketsch. Data represent mean and standard errors from 3 to 12 independent experiments with three individuals per experiment and genotype.

Table 1. Scoring scheme to evaluate disease severity after infection with *P. ampelicida* according to the EPPO standard PP1/4(4) for *Erysiphe necator* (EPPO 2020).

Category [%]	0	2.5	7.5	17.5	37.5	62.5	82.5	95
Definition [% coverage]	0	0–5	5–10	10–25	25–50	50–75	75–90	90–100

Observation of late development

We observed later development stages (>5 dpi) of mycelial growth, symptoms and pycnidia formation on entire leaves that were still attached to the plants. For this, plants were inoculated with a sprayer head (made of DURAN® tubing) in combination with an Erlenmeyer flask (Lenz Laborglasinstrumente, Wertheim, Germany) on the adaxial leaf surface until run-off, incubated for 24 h in a humid chamber to allow infection under wet conditions and cultivated as described above.

To validate translaminar growth of *P. ampelicida* in grape leaves, entire plants were tilted upside down to allow inoculation of the abaxial leaf surface without run-off of the inoculation droplets. A plastic bag placed over the pot and plant helped avoid loss of substrate. Then leaves 3 and 4 were marked and each leaf inoculated with ten droplets (20 µl) of spore suspension. To prevent evaporation of inoculation droplets and maintain high humidity, plants were covered with moistened plastic bags and incubated for 24 h. Plants were then cultured in the greenhouse in an upright position. Symptoms were evaluated 14 and 21 dpi. Data represent mean ± SE from three independent experiments, each with four biological replicates.

Visualization of early fungal development using histochemistry

Samples were collected at different time points after inoculation and stored in 25 ml 90% ethanol (for maximum 2 weeks at room temperature) to stop fungal development and remove chlorophyll. To avoid shrivelling of leaf discs during subsequent processing, we carefully added 50 ml distilled H_2O in 2-ml steps for about 30 min. Then leaf discs were transferred to 50 ml 1 M KOH and incubated at 80°C for at least 5 h to obtain transparent leaf discs. Attached conidia were stained with 0.05% w/v Direct Yellow 96 (diphenyl brilliant flavine 7 GGF) for 5 min, followed by three passages of rinsing with distilled water to remove excess dye. Appressoria and hyphae were stained with several drops of 0.05% (w/v) Aniline Blue (Keller, Mannheim, Germany) dissolved into 1 M Tris HCl, pH 10. All fungal structures were examined immediately using epi-fluorescence microscopy (Zeiss Axio Scope.A1; Kübler HXP-120C lighting device; filter set 05, excitation 395–440 nm, emission at 470 nm; software Axio Vision 4.8). Accumulation of phenols in those cells where conidia had attached was visualized with Methyl Red following Kortekamp *et al.* (1998) in destained leaf discs and visualized with bright-field microscopy.

Low temperature scanning electron microscopy (LTSEM)

Excised leaf pieces (*ca.* 0.5 cm^2) or entire leaves collected at specific time intervals were mounted on a specimen holder with graphite glue (Kolloidaler Graphit AQUADAG in water, Agar Scientific, Stansted, UK). Samples were first precooled in liquid nitrogen under vacuum before being transferred to the SEM (Stereo Scan S260, Leica, Bensheim, Germany). By adjusting to −80°C the condensed water was allowed to sublimate on the surface for 15 to 20 min. Subsequently, samples were sputter-coated with gold under an Argon atmosphere and investigated at an acceleration voltage of 15 kV. Images were recorded with the software 'diss' (Point Electronics, Halle, Germany).

Plate-assays for nutritional profiling

To evaluate the ability of *P. ampelicida* to use different plant components as carbon source, we designed a semi-quantitative plate assay, where minimal medium was complemented with the respective plant compound. The minimal medium consisted of 0.6% (w/v) $NaNO_3$, 0.15% (w/v) K_2HPO_4, 0.05% (w/v) KCl, 0.05% (w/v) $MgSO_4 \times 7\ H_2O$, 0.001% (w/v) $FeSO_4 \times 7\ H_2O$, 1.5% (w/v) agar and 0.1% (v/v) trace metal solution (1% (w/v) $ZnSO_4 \times 7\ H_2O$ and 0.5% (w/v) $CuSO_4 \times 5\ H_2O$). As supplements, we used 1% (w/v) of either carboxymethyl cellulose (CMC), xylan from beech wood (hemicellulose), or citric pectin in autoclaved agar, adjusted to pH 6.5. For pectin agar, two different acidity levels (pH 5 or pH 7) were used to address different types of pectin degrading enzymes. After inoculation with actively growing mycelium as described above, the plates remained at 25 °C under continuous light for 15 days. After which we scored fungal growth by measuring colony diameter. To detect the respective enzymatic activites for carbon mobilization, the plates were labelled histochemically, to produce a destained halo around the colony reporting the amplitude of enzyme activity. To detect cellulose and hemicellulose activity, we added Lugol's iodine (5% w/v iodine, 10% potassium iodide in water) for 5 min. Degradation of pectins by pectate lyases (pH 7) and polygalacturonases (pH 5) were visualized with 10 ml 10% cetyl trimethylammonium bromide (CTAB) for 40 min at 30 °C according to Hankin & Anagnostakis (1975). Data represent three independent experimental series with five technical replicates per data point.

Visualization of the plant defence response using histochemistry

Autofluorescence from accumulation of defence-related secondary compounds was followed in destained leaf discs, again using excitation in blue and emission in green (filter set 05, Zeiss Axio Scope.A1). Superoxide generated as a result of defence was visualized according to Doke (1983) with 0.5% w/v nitroblue tetrazolium in 0.1 M potassium phosphate buffer and observed with bright-field microscopy, classifying the response depending on intensity and area into five classes (Fig. 7A).

Statistical analysis

The quantitative data for infection frequency and severity (see above) were analysed using the XLSTAT plugin (Addinsoft, Paris, France) for Microsoft Excel. Data were tested for normality with the Shapiro–Wilk test. For data with normal distribution, significance of observed differences used ANOVA, before pairwise probing significance of differences with the Tukey Honest Significant Difference (HSD) test. For data deviating from a normal distribution, the non-parametric Kruskal–Wallis test was used instead of ANOVA. Pairwise differences were then analysed using the non-parametric Steel-Dwass-Critchlow-Fligner test. To test linearity between pathogenicity and efficiency of use of different carbon sources, a Pearson linear regression was employed.

RESULTS

Susceptibility to black rot depends on leaf maturation

To calibrate our experimental system, we first tested whether the susceptibility to Black Rot depends on leaf development. As experimental model, we used the susceptible *vinifera* variety 'Müller-Thurgau', which is economically relevant in south Germany. We inoculated entire plants, in a standardized manner, with a defined inoculum from *P. ampelicida* and scored symptom expression 3 weeks later for each individual leaf separately (Fig. 1A) down to leaf number 8, and up to leaf number −2, counted from the inoculation site (leaves that had been newly formed after inoculation were defined by a negative position). For the susceptible 'Müller-Thurgau', expression of symptoms (measured as percentage cover of symptomatic leaf areas) was maximal in the first two leaves basal to the inoculation site but declined strongly in the more mature leaves, fading out till leaf 7 (Fig. 1B). We compared this to the developmental course in two *sylvestris* genotypes, Ke18 and Ke38, which, during preparatory experiments, were found to be relatively resistant. Also here, symptoms declined with progressive age of the leaf. However, the decline was much steeper, such that leaf 3 was the last where significant symptoms were detectable. The infection of leaves incepted after inoculation (leaves −1 and −2, respectively) sharply declined as compared to leaf 1, which was already present at inoculation. This would be expected, since these leaves must have obtained their infection indirectly, *via* leaf 1. For this reason, we excluded these leaves from the comparison of genotypes (Figure S4). Thus, the susceptibility to Black Rot clearly depends on leaf maturation.

The transition from biotrophy to necrotrophy is marked by trans-laminar growth

To obtain insight into the early biotrophic development that allows the fungus to colonize large areas of the leaf without macroscopic symptom expression, we conducted a time course study based on controlled infection of the susceptible genotype *V. vinifera vinifera* cv. Müller-Thurgau with *P. ampelicida* and followed fungal development with SEM and fluorescence microscopy. Already 2 h post-infection (hpi) we could see attached pear-shaped conidia, so-called pyknospores, that had formed a germ tube (Fig. 2A) and fully stained with Direct Yellow, a general stain for fungal cell walls (Fig. 2B). Around 24 hpi, appressoria were fully melanized and the melanin quenched fluorescence of the cell wall, as visualized with Direct Yellow (Fig. 2B). We also could clearly discern up to two septae brightly stained with Aniline Blue (Fig. 2C). While the appressoria became fully turgescent, the pyknospores collapsed

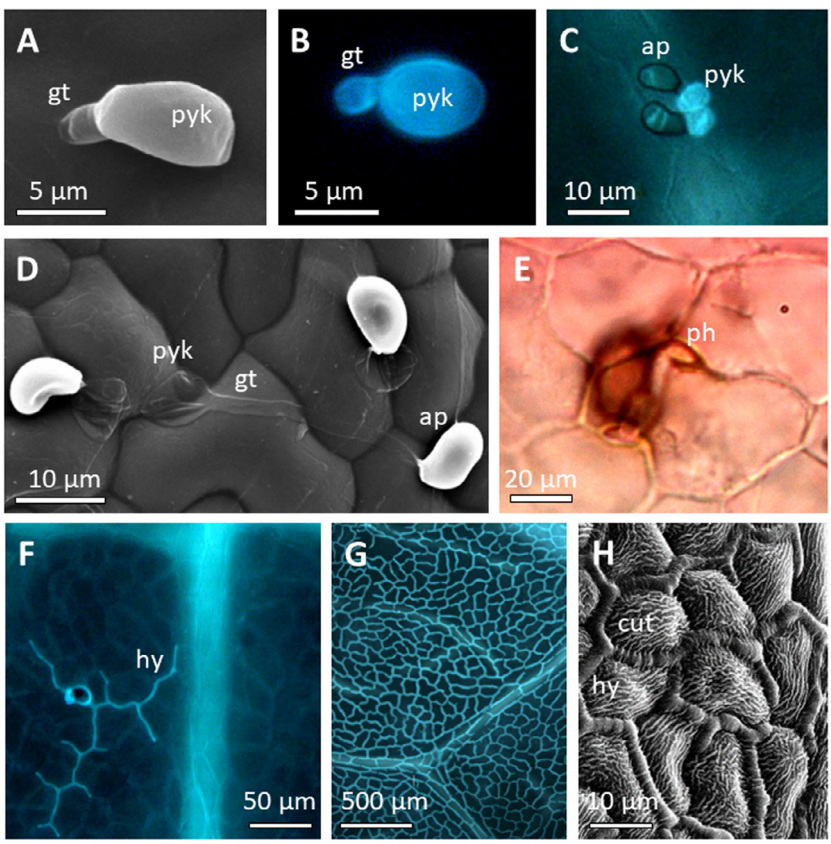

Fig. 2. Subsequent stages of the infection process on the adaxial leaf surface of the susceptible vinifera variety 'Müller-Thurgau'. (A, B) Pyknospores (pyk) that have formed a germ tube (gt) at 2 hpi visualized by SEM (A) or after fluorescent labelling with Direct Yellow (B). (C) Melanised appressoria (ap) at 24 hpi fluorescent by Aniline Blue. (D) Turgescent appressoria and collapsed pyknospores and germ tube at 24 hpi imaged by SEM. (E) Primary hypha (ph) at 48 hpi, visualized by Methyl Red and bright-field microscopy. (F) Hyphae at 5 dpi, fluorescently labelled by Aniline Blue. (G) Fully developed hyphal network at 10 dpi after staining with Aniline Blue. (H): Hyphal network at 10 dpi after imaging by SEM. The hyphae line the epidermal cells and grow underneath the cuticle (cut).

completely, leaving only the emptied cell wall, when viewed with SEM (Fig. 2D). Around 48 hpi, primary hyphae were stainable with Methyl Red (Fig. 2E). Soon after, branching hyphae with their characteristic alignment with host cell walls could be stained with Aniline Blue (Fig. 2F) that up to 10 dpi had fully colonized the surface of the leaf (Fig. 2G). With SEM the hyphae can be seen growing beneath the cuticle, following the anticlinal cell walls, but without entering the host cells (Fig. 2H). Cuticular folds align over neighbouring cells and cross the hyphae without any sign of discontinuity, which allowed us to follow the topology very clearly.

Once a substantial fraction of the leaf lamina has been colonized (depending on the conditions between 10–14 dpi), fungal development undergoes a transition from two-dimensional towards three-dimensional growth (Fig. 3). Upon staining with Aniline Blue, the mesh-like pattern with hyphal growth along cell edges change into larger structures that begin to protrude from the adaxial surface (Fig. 3A) and appear as globular structures in SEM (Fig. 3B). Later, melanized pycnidia appear (Fig. 3C), on a macroscopic level coinciding with the characteristic brown spots and patches (Fig. 3D) that underly the disease name (Black Rot). The pycnidium apex bulges out (Fig. 3E) and, during subsequent elongation, curls up (Fig. 3B). The pycnidia exclusively appear at the adaxial surface of the leaf, leading to the question of whether gravity might be used as a guiding cue. We therefore conducted an experiment where plants were infected on the abaxial side of the leaf, while the plant was placed upside down (Figure S1), and then fungal development allowed to proceed, with the plants returned to normal orientation once the inoculation droplet had dried (not shown in the figure). However, even under these conditions, symptoms developed only on the adaxial side of the leaf, demonstrating that three-dimensional growth is not directed by the site of infection, but by the innate asymmetry of the bifacial leaf. We also observed that the transition towards three-dimensional growth initiates at the periphery of the infection site (Fig. 3A). Since the pycnidia are usually also found at the periphery, they seem to derive from these early three-dimensional hyphae.

Specific clades in *V. Sylvestris* show elevated resistance to black rot

To probe for genetic components of Black Rot susceptibility, we conducted a systematic study with a collection of 82 genotypes of *V. vinifera* subsp. *vinifera* and subsp. *sylvestris*

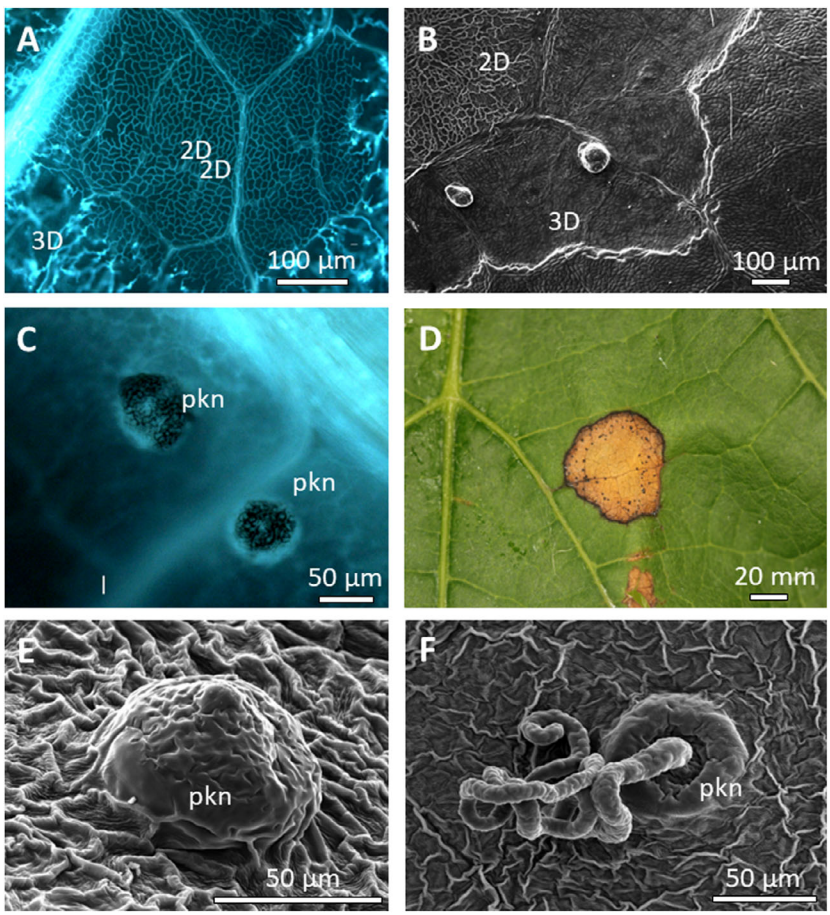

Fig. 3. Late stages of the infection process on the adaxial leaf surface of the susceptible vinifera variety 'Müller-Thurgau'. (A, B) Transition from two-dimensional (2D) towards three-dimensional (3D) hyphal growth at 11 dpi, visualized by fluorescent labelling with Aniline Blue (A) or SEM (B). (C) Melanised pyknidia (pkn) at 24 dpi fluorescent by Aniline Blue. D: Macroscopic appearance of a symptom spot. (E, F) young (E) and advanced (F) stages of pyknidia development at 23 dpi as visualized by SEM.

comprising most of the gene pool for subsp. *sylvestris* still remaining in Germany (Table S1). To validate the scoring parameters, we compared disease severity and disease incidence after controlled inoculation with *P. ampelicida* in leaves of two development stages – leaf 5 (just completing full expansion) and leaf 7 (full maturation of the leaf) for a set of 40 *sylvestris* genotypes and two *vinifera* varieties (Data S1). We found that severity and incidence correlated positively to a high degree ($R^2 > 0.8$), irrespective of whether leaf 5 (Figure S2A) or leaf 7 (Figure S2B) were analysed. Likewise, incidence in leaves 5 and 7 (Figure S3C), as well as severity in leaves 5 and 7 (Figure S2D) were positively and tightly ($R^2 > 0.9$) correlated. The high correlations confirms that both scoring parameters and both leaf tiers assessed for a genotype reported a very comparable readout for disease susceptibility of this genotype. Once this had been clarified, we assessed severity (Figure S3A,B) and incidence (Figure S3C,D) over the entire population, and found a wide range of variation. For instance, the lowest value for severity in genotype Ke16 was only 0.17, while it was more than two orders of magnitude higher (24.1) in genotype Ke108. For a subset of 28 *sylvestris* genotypes the entire genomes had been sequenced and used to infer the phylogenetic relationship (Liang *et al.* 2019). This subset could be assigned to five different clades (Fig. 4A). Compared to the tested three *vinifera* varieties (Müller-Thurgau, Augster Weiß, Regent), most (84%), but not all *sylvestris* genotypes of this set performed better for both disease severity (Figure S3A) and disease incidence (Figure S3B). However, the values within a given clade were also variable. We therefore pooled the genotypes from each clade and calculated the averages for incidence in leaf 5 (Fig. 4B) and leaf 7 (Fig. 4C). This revealed that the genome-sequenced subset of *sylvestris* accessions fell into two groups. While clades B and E were only moderately more resistant to Black Rot as compared to the commercially relevant *vinifera* variety Müller-Thurgau, clades A, C and D were significantly more resistant, with values that were less than 20% of those seen in Müller-Thurgau. Interestingly, the incidence in clade E, which was close to that in clade B for leaf 5, dropped somewhat with age, such that for leaf 7 the value for clade E was intermediate between that for clade B and those for the resistant clades A, C and D. In summary, there is considerable genetic variation in the *sylvestris* population with respect to Black Rot susceptibility. Particular clades of this population (A, C and D) show a strong reduction in susceptibility as compared to other clades (B and E), and even more pronounced, as compared to the *vinifera* variety Müller-Thurgau.

Hyphal elongation is impaired in resistant genotypes of *Vitis sylvestris*

To address the potential reasons behind the partial resistance of many of the *V. sylvestris* genotypes, we followed early development of *P. ampelicida* on different grapevine hosts in a comparative time course experiment, quantifying different aspects of fungal development (Fig. 5). In addition to the highly susceptible commercial variety Müller-Thurgau, we used the partially resistant hybrid Solaris (derived from introgression of various North American wild grapevines and the Siberian species *V. amurensis* into *V. vinifera*) and the rootstock variety (Börner), which is also highly resistant. This was compared to the resistant *sylvestris* genotypes Ke16, Ke18 (Figure S3B,D), and Ke38 (Figure S3A,C) on young, but fully expanded, leaves

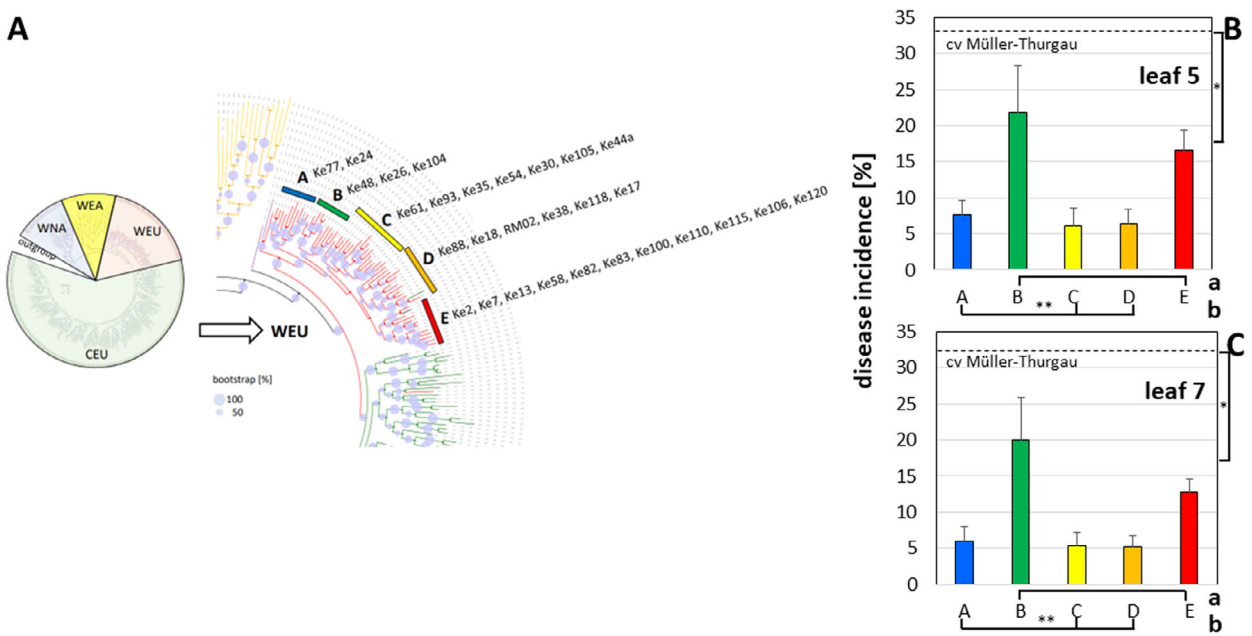

Fig. 4. Correlation between susceptibility (measured as disease incidence in the comparative infection assay) and phylogenetic relationship. (A) Phylogenetic tree constructed by Maximum Likelihood of the genome wide Single Nucleotide Polymorphisms (Liang *et al.* 2019) and definition of the different clades of the German sylvestris population. (B, C) Disease incidence for the representatives of the different clades in leaf 5 (B) and leaf 7 (C). Data represent mean values and standard errors from two independent infection series including three individuals per genotype. Brackets indicate highly significant (**$P < 0.01$) differences between clades (A), (C) and (D) *versus* clades (B) and (E). Clades (B) and (E) are, in turn, significantly (*$P < 0.05$) less affected than Müller-Thurgau. Colours of the bars correspond to the clades shown in (A).

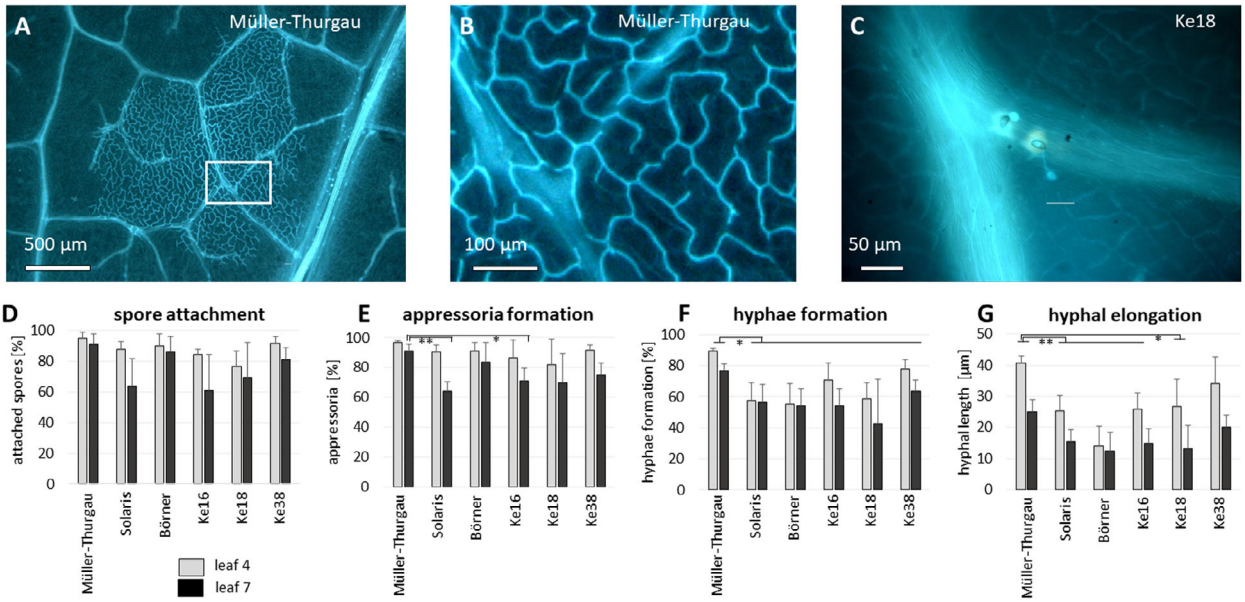

Fig. 5. Analysis of colonization on different host genotypes. A–C: Representative images of fungal development at 8 dpi on the vinifera variety Müller-Thurgau (A, zoom-in of the region highlighted in A is shown in B) or on the sylvestris genotype Ke18 (C) visualized by Aniline Blue. (D–G) Quantification of subsequent developmental events on the different genotypes on leaves that have just completed expansion (leaf 4, grey) and fully mature leaves (leaf 7, black). Data represent two independent infection series with five individual plants per genotype and experiment. Significant differences indicated by brackets, $*P < 0.05$, $**P < 0.01$, *t*-test.

(leaf 5) and matured leaves (leaf 7). In fact, while leaves of Müller-Thurgau were fully colonized at 8 dpi (Fig. 5A, B), only few strongly retarded infection structures were seen on Ke18 (Fig. 5C). When the progression through development was scored, we did not observe any significant differences with respect to spore attachment, neither for leaf 5 nor for leaf 7 (Fig. 5D). For appressorium formation, there was a slight, but significant, reduction on Solaris and Ke16, but only for the older leaves (Fig. 5E). Formation of hyphae was, instead, significantly reduced on all hosts but Müller-Thurgau, irrespective of leaf age, albeit only by around 10–20% (Fig. 5F). The clearest difference was observed for hyphal elongation (Fig. 5G). Here, the inhibition reached 40% in leaf 5 (for Ke16 and Ke18), and for leaf 7 was as low as in the highly resistant genotype Börner. Instead for Ke38, which, during later stages showed strongly reduced disease incidence and severity (Figure S3A,C), the reduction in elongation, although visible, had still not crossed the threshold for significance. Thus, the elongation of hyphae seems to be a sensitive target, where resistance depends on which side of the host is attacked.

Phyllosticta ampelicida can efficiently use pectins as carbon source

Since the fungus, during its biotrophic phase, grows along cell borders, apparently without the need to form haustoria, we hypothesized that it might use pectins as carbon source. To address this, we developed a plate assay, where defined inocula were allowed to grow on minimal medium complemented by different carbon sources, using the ratio of final colony size over initial inoculum as readout for growth. In addition to colony size, we also measured the size of the depletion zone for the respective carbon source around the colony (Fig. 6). Compared to the full medium, growth on the minimal medium was strongly reduced (Fig. 6A B). The growth factor dropped from almost 9 to 1.3 (Fig. 6J). When the minimum medium was complemented with starch (Fig. 6C), growth was rescued only slightly to a factor of 2.2 (Fig. 6J), also seen from the small depletion zone (Fig. 6C). Likewise, cellulose (Fig. 6D), carboxy-methylated cellulose (Fig. 6E,J), xylane (Fig. 6F,J) and tannic acid (Fig. 6I,J) were poor substrates for *P. ampelicida*. In contrast, pectin was able to sustain fungal growth, especially at acidic pH (Fig. 6G,H). Here, almost half of the growth found in the full media could be recovered (Fig. 6J). Thus, this plate assay would support a scenario, where *P. ampelicida*, during its biotrophic phase, can use the pectins of the middle lamellae as food source.

Partial resistance of *V. Vinifera* subsp. *sylvestris* correlates with swift oxidative burst

To probe for potential differences in the plant defence response, we visualized oxidative burst in response to inoculation with *P. ampelicida*. We stained with Nitroblue Tetrazolium (NTB), reporting superoxide anions generated by the membrane-located NADPH oxidase Respiratory burst oxidase Homologue (RboH), a central input for defence signalling. Using a histochemical classification system (Fig. 7A), we observed a strong increase in signal on infected leaves of the resistant *vinifera* genotype Solaris, and the partially resistant *sylvestris* genotypes Ke16, Ke18 and Ke38 from 24 h after infection, while no such indication for oxidative burst was seen in the susceptible Müller-Thurgau. Interestingly, also the highly resistant rootstock variety Börner did not deploy any response indicative of a different type of resistance, not depending on oxidative burst.

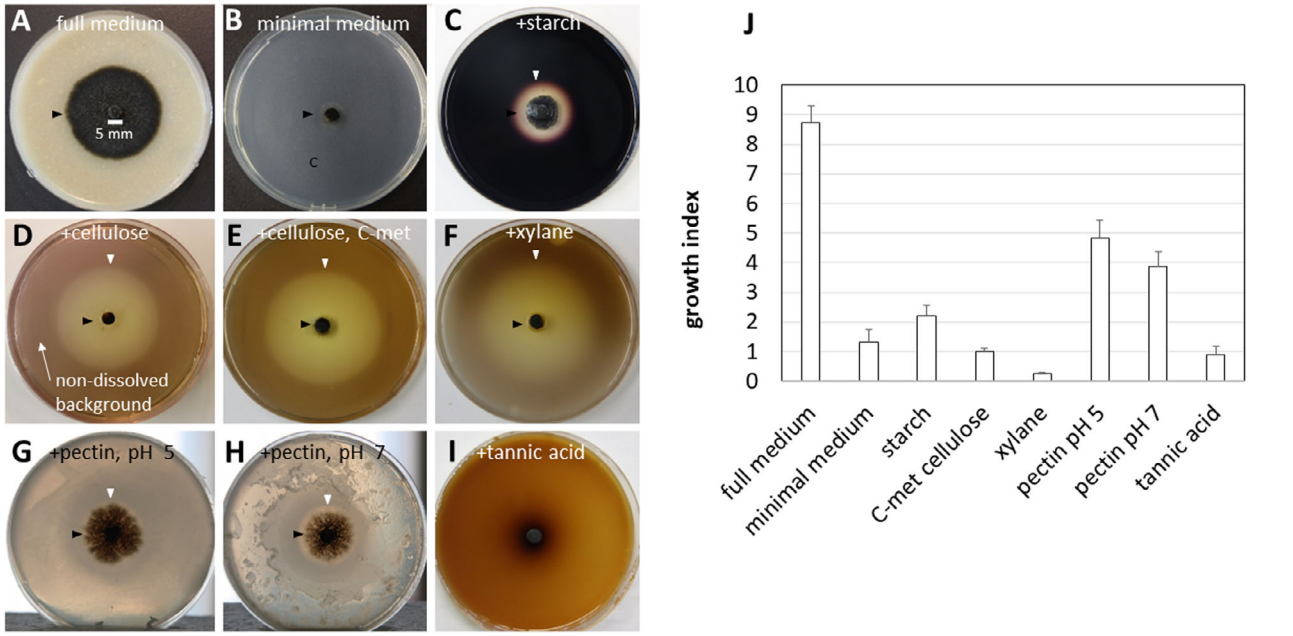

Fig. 6. Analysis of mycelium growth on minimal medium supplemented by different carbon sources (B–I), as compared to oat meal agar as full medium (A). Black arrowheads indicate the margin of the colony, white arrowheads indicate the substrate depletion zone. The diameter of the source inoculum was 5 mm. Note the whitish hue in (D, cellulose) indicating limited solubility of this substrate in the agar. (J) Quantification of growth (relative to the size of the initial inoculum) on different substrates. Cellulose was not measured due to the solubility problems (shown in D). Data represent three independent inoculation series with three individual plates per substrate.

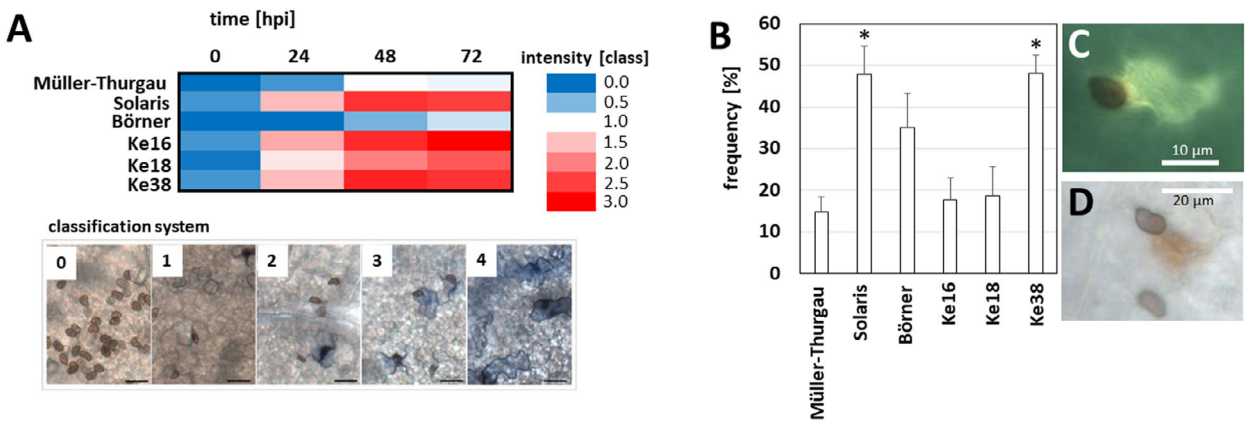

Fig. 7. Defence reactions of different host genotypes. (A) Time course for the accumulation of superoxide at the infection site as reported by NBT staining using a classification system with five classes. Data represent three experimental series each in five biological replications. (B) Frequency of appressoria (as percentage of all appressoria) that had induced autofluorescence in the surrounding host tissue, scored at 5 dpi. Data represent mean and standard errors from 8 individual plants. * represent significant differences from MüllerThurgau based on a Kruskal-Wallis test ($P < 0.05$). Representative examples of the host reactions are shown in (C, autofluorescence, host Börner) and (D, bright-field, host Ke38).

The activation of the phenylpropanoid pathway belongs to the central metabolic responses in grapevine. The resulting phenolic compounds show autofluorescence in blue. We checked, therefore, whether the cells surrounding a penetration site displayed autofluorescence and scored the frequency of these cells as readout for a metabolic defence response (Fig. 7B). Again, there was wide variation in the amplitude of this response, with high values of ~50% for Solaris and Ke38, closely followed by Börner. Instead, Müller-Thurgau and the two *sylvestris* varieties Ke16 and Ke18 exhibited a low frequency of autofluorescent penetration sites, <20%.

Thus, the profiles for oxidative burst and accumulation of autofluorescent compounds are not always congruent, such that we can discern four response types. Type A (Müller-Thurgau) lacks both oxidative burst as well as a metabolic response and is susceptible. Type B (Börner) lacks oxidative burst but shows a strong metabolic response and is resistant. Type C (Ke 16, 18) produce a strong oxidative burst, which is not followed by accumulation of phenolic compounds; this type is not able to contain the pathogen. Type D (Solaris, Ke38) produces both superoxide and phenolic compounds, to a considerable degree, and is also resistant. While we can

distinguish three response patterns associated with resistance to *P. ampelicida*, it is clear that at least one of the two scored defence responses needs to be deployed if the genotype were to be resistant.

DISCUSSION

Black Rot, caused by the Ascomycete *P. ampelicida*, has been introduced to Europe from North America, similarly to Downy Mildew and Powdery Mildew, but it has not acquired the same degree of attention. Nevertheless, this disease is an issue in organic viticulture and has progressively spread over vineyards in Europe, leading to the question whether genetic resources endowed with at least partial resistance to Black Rot might serve as starting point for resistance breeding, a strategy that has been successful in the case of Downy and Powdery Mildew. In fact, we can show partial resistance of some *V. vinifera sylvestris* hosts, which is linked with swifter progression of leaf development, leading to impaired hyphal elongation. We propose a model, where maturation of cell walls limiting energy foraging of the fungus contributes to partial resistance to Black Rot.

The above findings lead to the following questions, which are discussed below: What did we learn on the cellular factors associated with the colonization process? What is the reason behind the reduced hyphal elongation in the resistant *sylvestris* genotypes, is it a consequence of a more vigorous defence response, or is it linked with maturation processes of the cell wall? How do our findings contribute to novel strategies to manage Black Rot?

The first day is decisive and pectins are the crucial factor

The epidemic spread of Black Rot is mainly decided by the asexual infection cycle of *P. ampelicida* during a rainy May or June, facilitating the release of pycnidiospores from pycnidia after contact with water. The early steps of infection, from the attachment of pycnidiospores, their germination, the formation of appressoria, until final development of hyphae, have therefore attracted attention in several studies in the 1990s. Our observations basically confirm and extend previous findings (Kuo & Hoch 1995, 1996a,b), with a few exceptions. We did not observe the apical appendages of the pycnidiospores described earlier (Sivanesan & Holliday 1981; Kuo & Hoch 1996b), no matter whether we used brightfield or fluorescence microscopy, which is congruent with Ullrich *et al.* (2009), working with the same isolate as in our study. Thus, the validity of these appendages as diagnostic trait to assign a fungus to the genus *Phyllosticta* (van der Aa 1973) must be questioned. We rather concur with Wikee *et al.* (2013), that these appendages are not a common trait for *Phyllosticta*, since several species, such as *P. colocasiicola*, *P. minima* or *P. sphaeropsoidea*, are devoid of them, as was the case in our strain.

Other cellular details of early development described by Kuo & Hoch (1996b) could be confirmed, such as the formation of appressoria at the apical end of the germ tube, the preferential formation of appressoria at short germ tubes, or the collapse of the pycnidiospore after the successful establishment of an appressorium, as well as growth under the cuticle along anticlinal walls. However, we were also able to discern details not reported previously. For instance, we could observe septa within the appressoria. Such septa had been indicated by an apparent delineation between germ tube and appressorium (Shaw *et al.* 1998), but not confirmed during a subsequent study using transmission electron microscopy. Possible reasons for the discrepancy between our study and that of Shaw *et al.* (1998) might be geographic origin (Germany *versus* North America) and the conditions of appressoria formation (natural host surface *versus* a synthetic polycarbonate surface).

The current study allowed new insights into the transition towards necrotrophy taking place around day 12 post-infection. Whereas it was not possible to directly observe, using fluorescence microscopy, which host cell layers were involved, we could show using an inverted infection set-up, where we inoculated the abaxial side of the leaf, that the pycnidia were found on the adaxial side, which also shows that the pathogen is capable of colonizing all cell layers of the leaf.

A peculiar aspect of *Phyllosticta* colonization is the hyphal growth above anticlinal walls. While subcuticular intramural growth has been reported for *Colletotrichum* on certain hosts (Perfect *et al.* 1999), there is no endophytic stage, since the hyphae of *Colletotrichum* quickly penetrate the host cells (Curry *et al.* 2002; Diéguez-Uribeondo *et al.* 2005). Likewise, other pathogens with subcuticular mycelia, such as apple (*Venturia inaequalis*) or pear scab (*Venturia nashicola*) differ in lacking any preference for anticlinal cell walls (Sivanesan *et al.* 1974; Park *et al.* 2000; Jiang *et al.* 2007). The reason for this anticlinal pattern of *P. ampelicida* is unknown but might be linked with nutrient uptake. Previous work has proposed uptake of pectins (Kuo & Hoch 1996b), or sugars and amino acids (Ullrich *et al.* 2009). The lack of any haustoria suggests that *P. ampelicida* forages energy in a manner similar to *Venturia inaequalis*, where haustoria are also absent, but energy is recruited through the controlled release of cell wall degrading enzymes (Jha *et al.* 2009). This hypothesis is supported by the data from our plate assay, demonstrating clearly that *P. ampelicida* is able to efficiently use pectins as carbon source. The fact that pectin can be mobilized both at acidic and neutral pH indicates that *P. ampelicida* has command of both polygalacturonidases and pectolyases (Hankin & Anagnostakis 1975). Thus, the strategy seems to be similar to that of *V. inaequalis*, which first perforates the cuticle *via* cutinases (Köller *et al.* 1991), and then secretes endopolygalacturonases (Kollar 1998), as well as cellulases (Kollar 1994) to recruit carbon from the host cell wall (Jha *et al.* 2009). The formation of appressoria and concomitant transfer of cytoplasm from the collapsing germtubes is a rapid process and can be seen as early as 24 hpi, directly followed by the emergence of primary hyphae that already align with the anticlinal walls. This time window seems to be decisive for the success of colonization because the penetration of the cuticle by the appressorium must be swiftly followed by the mobilization of carbon through breakdown of pectins so as to sustain the rapid elongation of the hyphae.

Why leaves of *sylvestris* might be more resistant to black rot

The comparative study of fungal development on the susceptible Müller-Thurgau, as compared to the resistant *sylvestris* genotypes Ke16, Ke18 and Ke38, pinpointed hyphal elongation as crucial step. Instead, all the early stages of development did not reveal any significant differences. In other words, the

partial resistance of the *sylvestris* genotypes becomes manifest during the phase when the hypha aligns with the anticlinal walls of the host epidermis. This might be linked with the use of pectins as carbon source (with the caveat that this was assessed in a host-free system and only with one field isolate of the pathogen). As pointed out above, this is the time when the fungus most likely uses wall pectins as carbon source. Changes in the chemistry of the cell wall occurring during the maturation of leaves are expected to impair the recruitment of pectins and, thus, to inhibit hyphal elongation. In fact, *P. ampelicida* is only efficient in young leaves, progressively losing momentum as the leaves mature. This age-dependent resistance is progressing faster in *sylvestris* as compared to Müller-Thurgau, which is correlated with a slower expansion and faster differentiation of leaves in *V. sylvestris* as compared to *V. vinifera* in general and to Müller-Thurgau in particular. In fact, the transition from expansion to maturation is linked with changes in cell wall chemistry in grapevine. The main components of fully expanded leaves are xyloglucans (Moore *et al.* 2014). Since these polysaccharides can form hydrogen bonds with cellulose microfibrils they cause a rigidification of the cell wall and, thus, restrict cell expansion (Levy *et al.* 1991). Pectins, which are produced as methyl esters, are demethylated in the cell wall and, thus, acquire a negative charge. The demethylated form is predominant in rapidly expanding cells (Haas *et al.* 2020). Thus, leaf development is accompanied by an increase of xyloglucans and a decrease of pectins in the cell wall. We are currently following changes in cell wall chemistry over development, and preliminary data show that pectins are progressively modified by phenolic compounds, such as ferulic acid. In other words: maturation impairs the suitability of grapevine leaves as food source for *P. ampelicida*. Since leaves of *V. sylvestris* expand not over the same time span as leaves of Müller-Thurgau, they are expected to sustain infection less efficiently, and this resistance should be age-dependent. Both implications are clearly confirmed by our data.

Faster leaf maturation as resistance factor does not exclude that resistance might also be linked by a swifter and more vigorous defence response. In fact, the three *V. sylvestris* genotypes Ke16, Ke18 and Ke38 did not only show good resistance against *P. ampelicida*, but accumulated the highest NBT signal, reporting accumulation of superoxide around the penetration site. Apoplastic superoxide is generated by the plasma membrane-located NADPH oxidase Respiratory burst oxidase Homologue (RboH), a central input for stress signalling (Marino *et al.* 2012). In grapevine cells, activation of RboH has been observed in response to elicitor-triggered defence, whereby the time course differs between basal and cell death-related immunity (Chang & Nick 2012). Thus, the tested *sylvestris* genotypes are not only less palatable for the hyphae, because their cell walls become more rapidly depleted of pectin as central carbon source for the fungus, but also because they can more efficiently deploy a defence response. Whether this is linked with a higher abundance of chitin receptors (Sofi *et al.* 2023) or with more active expression of RboH is not known, but represents a rewarding research topic for the future. A scenario, where the partial resistance of *V. sylvestris* stems from R-genes against *P. ampelicida* is highly unlikely, because R-genes derive from a long history of co-evolution between host and pathogen. While R-genes might be expected among wild grapevine species from North America, they are certainly absent from a naïve host, such as *V. sylvestris*, considering that this pathogen was first detected in Europe as late as 1885.

What can we do with this knowledge?

Our study has produced two outcomes that are relevant for application. First, we identified maturation of cell wall composition relevant for hyphal elongation during the biotrophic phase as contributing to resilience against Black Rot. Second, we identified genotypes in the ancestral species *Vitis sylvestris* with improved resilience. On the basis of these outcomes, two strategies for containment of this disease can be envisaged: agricultural practices that promote leaf maturation are expected to mitigate infection pressure, because the time window for infection would be reduced. Here, light and fertilization, especially micronutrients, are of interest. For instance, supply of boron as cross-linker for rhamnogalacturonan moieties in the cell wall is limiting for maturation (Matoh & Kobayashi 1998), such that supplementation with boron might support Black Rot resilience. Leaf expansion is strongly dependent on light and more pronounced under shade as compared to higher light intensity (for a classical review see Lichtenthaler *et al.* 1981). Thus, improving penetration of light into the canopy should promote leaf maturation – this could be steered by adjusting the pruning, the spacing of plants, but also by moderate defoliation of the upper leaf tiers. The identification of *sylvestris* genotypes with improved resilience could be validated to launch introgression strategies of these resilience factors into commercial varieties. A similar strategy had been used to introduce resistance factors against Downy and Powdery Mildew from North American and Siberian wild grapevine species into *V. vinifera*, giving rise to so called 'PiWi' (for *Pilz-Widerstandsfähig*, fungal resistance) varieties that have become an important factor in organic viticulture in south Germany. Such introgression strategies have been strongly accelerated by marker-assisted breeding (for review see Eibach *et al.* 2007). A drawback of this strategy has been the specific flavour, so-called foxiness, especially of the North American donors for this resistance. While it was possible to partially eliminate this by repeated backcrossing into *V. vinifera*, the resulting varieties, while becoming definitely palatable, still suffer from a lower consumer acceptance compared to classical varieties. In case of the *sylvestris* genotypes identified during our study, this problem is expected to be far less pronounced, since the resistance donor comes from the same species (*V. vinifera*) as the recipient. Moreover, numerous varieties, including the commercially relevant Riesling, derived from large-scale introgression of *V. vinifera sylvestris* parents into a *V. vinifera vinifera* background. Such introgression strategies would profit strongly from identification of the genetic factors underlying the resilience to Black Rot – this could be achieved by unbiased searches, for instance through GWAS, or by specifically analysing candidate factors involved in cell wall maturation. In the meantime, almost the entire *sylvestris* germplasm has been sequenced and organized into a searchable genome database, GrapeKIT (http://mygeninformatics.com). In combination with crossing populations of the resilient genotypes identified in the current study, this would allow us to identify and utilize genetic factors for the breeding of Black Rot resistant varieties. However, it is not sufficient to exclusively focus on the host. The current study is based on one field isolate found in Germany. The region of pathogen origin,

North America, might harbour other strains with substantially altered infection behaviour, as we had seen earlier for *Plasmopara viticola*, another important grapevine pathogen (Schröder *et al.* 2011). For the sake of resistance management, a better knowledge of pathogen evolution is mandatory.

ACKNOWLEDGEMENTS

This work was supported by the German Federal Agency for Agriculture (Programme for Sustainable Agriculture, BÖLN), and the BACCHUS Interreg IV Upper Rhine project co-financed by the European Union/European Regional Development Fund (ERDF). We gratefully acknowledge Joachim Daumann and Kerstin Huber (Karlsruhe Institute of Technology) for taking care of the *Vitis sylvestris* collection at the JKIP Experimental Station. Open Access funding enabled and organized by Projekt DEAL.

SUPPORTING INFORMATION

Additional supporting information may be found online in the Supporting Information section at the end of the article.

Data S1. Incidence and severity of Black Rot symptoms upon controlled inoculation of different accessions of *Vitis sylvestris* along with *V. vinifera* varieties.

Table S1. Identity and origin of the grapevine accessions used in this study.

Figure S1. Experimental set-up to demonstrate that three-dimensional growth is not guided by the gravity vector, but by the bifaciality of the leaf. Inoculation was administered to the abaxial face of the leaf (left) and plants were kept inverted such that the gravity vactor was opposing leaf dorsiventrality (centre). Neverthesless, symptoms developed at the adaxial face (right), even though this face of the leaf was oriented downwards.

Figure S2. Quantitative comparison of the response to standardised infection with *P. ampelicida* in a population of 40 *V. sylvestris* genotypes along with the two *vinifera* varieties Muller-Thurgau and Augster WeiB assessed at 21 dpi showing the correlations of disease severity (quantified as leaf coverage) upon disease incidence (quantified as frequency of leaves showing symptoms) in leaf 5 (A), in leaf 7 (B), the correlation between incidence in leaf 7 upon the incidence in leaf 5 of the same plant (C), and the correlation of disease severity in leaf 7 upon severity in leaf 5 of the same plant (D).

Figure S3. Genetic variation of disease severity (measured as % coverage in the comparative infection assay) and infection frequency (measured as fraction of symptomatic leaves irrespective of symptom severity). (A) Disease everity in commercial varieties of V. *vinifero* versus accessions of *V. sylvestris* of known phylogenetic position (as defined in Fig. 4). (B) Variation of disease severity in accessions of *V. sylvestris* of unknown phylogenetic position. (C) Infection frequency in commercial varieties of *V. vinifero* versus accessions of *v. sylvesrris* of known phylogenetic position (as defined in Fig. 4). (D) Variation of infection frequency in accessions of *V. sylvestris* of unknown phylogenetic position. Data represent mean and standard error from 3·to 12 independent experiments with three individuals per experiment.

REFERENCES

van der Aa H.A. (1973) Studies in *Phyllosticta*. I. *Studies in Mycology*, **5**, 1–110.

Chang X., Nick P. (2012) Defence signalling triggered by Flg22 and harpin is integrated into a different stilbene output in vitis cells. *PLoS One*, **7**, e40446.

Curry K.J., Abril M., Avant J.B., Smith B.J. (2002) Strawberry anthracnose: histopathology of *Colletotrichum acutatum* and *C. fragariae*. *Phytopathology*, **92**, 1055–1063.

Diéguez-Uribeondo J., Förster H., Soto-Estrada A., Adaskaveg J. (2005) Subcuticular-intracellular hemibiotrophic and intercellular necrotrophic development of *Colletotrichum acutatum* on almond. *Phytopathology*, **95**, 751–758.

Doke N. (1983) Generation of superoxide anion by potato tuber protoplasts during the hypersensitive response to hyphal wall components of *Phytophthora infestans* and specific inhibition of the reaction by suppressors of hypersensitivity. *Physiological Plant Pathology*, **23**, 359–367.

Eibach R., Zyprian E., Welter L., Töpfer R. (2007) The use of molecular markers for pyramiding resistance genes in grapevine breeding. *Vitis*, **46**, 120–124.

European and Mediterranean Plant Protection Organization (2020) EPPO Standards – PP1 Efficacy evaluation of plant protection products. Available from https://www.eppo.int/RESOURCES/eppo_standards/pp1_list (accessed 1 April 2022)

Galet P. (1977) *Les Maladies et les Parasites de la Vigne: les champignons et les Virus*. Paysan du Midi, Montpellier, France.

Gessler C., Blaise P., Jermini M. (2006) Blackrot on the hybrid vitis cultivar Isabella. *Integrated Protection in Viticulture*, **29**, 95–102.

Gessler C., Pertot I., Perazzolli M. (2011) *Plasmopara viticola*: a review of knowledge on downy mildew of grapevine and effective disease management. *Phytopathologia Mediterranea*, **50**, 3–44.

Haas K.T., Wightman R., Meyerowitz E.M., Peaucelle A. (2020) Pectin homogalacturonan nanofilament expansion drives morphogenesis in plant epidermal cells. *Science*, **367**, 1003–1007.

Hankin L., Anagnostakis S. (1975) The use of solid media for detection of enzyme production by fungi. *Mycologia*, **67**, 597–607.

Harms M., Holz B., Hoffmann C., Lipps H., Silvanus W. (2005) Occurrence of *Guignardia bidwellii*, the causal fungus of black rot on grapevine, in the vine growing areas of Rhineland-Palatinate, Germany. *BCPC Symposium Proceedings*, **81**, 127–132.

James P., Steger M.B. (2014) A genealogy of 'Globalization': the career of a concept. *Globalizations*, **11**, 417–434.

Jermini M., Angst A., Raynal M., Gessler C., Broggini G. (2009) First study on the population genetic structure of *Guignardia bidwellii*. In: Calonnec A., Gessler C., Kassemeyer H.H., Maixner M., Thiéry D., Zahavi T. (Eds), *IOBC-WPRS Working Group integrated protection and production in viticulture*, Vol. **67**. Staufen im Breisgau, Germany, pp 143–148.

Jha G., Thakur K., Thakur P. (2009) The *Venturia* apple pathosystem: pathogenicity mechanisms and plant defense responses. *Journal of Biomedicine & Biotechnology*, 680160.

Jiang S., Park P., Ishii H. (2007) Ultrastructural study on scab resistance expressed in epidermal pectin layers of pear leaves. *Journal of General Plant Pathology*, **73**, 314–323.

Kollar A. (1994) Characterization of specific induction, activity, and isozyme polymorphism of extracellular cellulases from *Venturia inaequalis* detected *in vitro* and on the host plant. *Molecular Plant-Microbe Interactions*, **7**, 603–611.

Kollar A. (1998) Characterization of an endopolygalacturonase produced by the apple scab fungus, *Venturia inaequalis*. *Mycological Research*, **102**, 313–319.

Köller W., Parker D.M., Becker C.M. (1991) Role of cutinase in the penetration of apple leaves by *Venturia inaequalis*. *Phytopathology*, **81**, 1375–1379.

Kortekamp A., Wind R., Zyprian E. (1998) Investigation of the interaction of *Plasmopara viticola* with susceptible and resistant grapevine cultivars. *Journal of Plant Diseases and Protection*, **105**, 475–488.

Kuo K., Hoch H. (1995) Visualization of the extracellular matrix surrounding pycnidiospores, germlings, and appressoria of *Phyllosticta ampelicida*. *Mycologia*, **87**, 759–771.

Kuo K., Hoch H. (1996a) Germination of *Phyllosticta ampelicida* Pycnidiospores: prerequisite of adhesion to the substratum and the relationship of substratum wettability. *Fungal Genetics and Biology*, **20**, 18–29.

Kuo K., Hoch H. (1996b) The parasitic relationship between *Phyllosticta ampelicida* and *Vitis vinifera*. *Mycologia*, **88**, 626–634.

Lee T.H., Guo H., Wang X., Kim C., Paterson A.H. (2014) SNPhylo: a pipeline to construct a phylogenetic tree from huge SNP data. *BMC Genomics*, **15**, 162.

Levy S., York W.S., Stuike-Prill R., Meyer B., Staehelin L.A. (1991) Simulations of the static and dynamic molecular conformations of xyloglucan: the role of the fucosylated sidechain in surface-specific sidechain folding. *The Plant Journal*, **1**, 195–215.

Liang Z.C., Duan S.C., Sheng J., Zhu S.S., Ni X.M., Shao J.H., Liu C.H., Nick P., Du F., Fan P.G., Mao R.Z., Zhu Y.F., Deng W.P., Yang M., Huang H.C., Liu Y.X., Ding Y.Q., Liu X.J., Jiang J.F., Zhu Y.Y., He X.H., Chen W., Li S.H., Dong Y. (2019) Whole-genome resequencing of 472 Vitis accessions for grapevine diversity and demographic history analyses. *Nature Communications*, **10**, 1190.

Lichtenthaler H.K., Buschmann C., Döll M., Fietz H.-J., Bach T., Kozel U., Meier D., Rahmsdorf U. (1981) Photosynthetic activity, chloroplast ultrastructure and leaf characteristics of high-light and low-light plants and of sun and shade leaves. *Photosynthesis Research*, **2**, 115–141.

Lipps H., Harms M. (2004) Schwarzfäule – Ein neues Problem. *Das Deutsche Weinmagazin*, **11**, 10–13.

Loskill B., Molitor D., Koch E., Harms M., Berkelmann-Löhnertz B., Hoffmann C., Kortekamp A., Porten M., Louis F., Maixner M. (2010) Strategien zur Regulation der Schwarzfäule (*Guignardia bidwellii*) im ökologischen Weinbau. *Deutsche Pflanzenschutztagung*, **57**, 375–376.

Marino D., Dunand C., Puppo A., Pauly N. (2012) A burst of plant NADPH oxidases. *Trends in Plant Science*, **17**, 9–15.

Matoh T., Kobayashi M. (1998) Boron and calcium, essential inorganic constituents of pectic polysaccharides in higher plant cell walls. *Journal of Plant Research*, **111**, 179–190.

Moore J.P., Nguema-Ona E., Fangel J.U., Willats W.G., Hugo A., Vivier M.A. (2014) Profiling the main cell wall polysaccharides of grapevine leaves using high-throughput and fractionation methods. *Carbohydrate Polymers*, **99**, 190–198.

Park P., Ishii H., Adachi Y., Kanematsu S., Ieki H., Umemoto S. (2000) Infection behavior of *Venturia nashicola*, the cause of scab on Asian pears. *Phytopathology*, **90**, 1209–1216.

Perfect S.E., Hughes H.B., O'Connell R.J., Green J.R. (1999) *Colletotrichum*: a model genus for studies on pathology and fungal–plant interactions. *Fungal Genetics and Biology*, **27**, 186–198.

Pezet R., Jermini M. (1989) Le Black-Rot de la vigne: symptômes, épidémiologie et lutte. *Revue Suisse de Viticulture, d'Arboriculture et d'Horticulture*, **21**, 27–34.

Ramsdell D.C., Milholland R.D. (1988) Black Rot. In: Pearson R.C., Goheen A.C. (Eds), *Compendium of Grape diseases*. American Phytopathological Society, St. Paul, MN, USA, pp 15–17.

Rex F. (2012) Resistenz gegen die Schwarzfäule (*Guignardia bidwellii*) in der Weinrebe (*Vitis spec.*) – Etablierung phänotypischer Erfassungsmethoden und genetische Kartierung von Resistenzloci. PhD Dissertation, Karlsruhe Institute of Technologie, Karlsruhe (Germany).

Schröder S., Kortekamp A., Heene E., Daumann J., Valea I., Nick P. (2015) Crop wild relatives as genetic resources – The case of the European Wild Grape. *Canadian Journal of Plant Science*, **95**, 905–912.

Schröder S., Telle S., Nick P., Thines M. (2011) Cryptic diversity of *Plasmopara viticola* (Oomycota, Peronosporaceae) in North America. *Organisms, Diversity and Evolution*, **11**, 3–7.

Shaw B.D., Kuo K., Hoch H.C. (1998) Germination and appressorium development of *Phyllosticta ampelicida* Pycnidiospores. *Mycologia*, **90**, 258–268.

Sivanesan A., Holliday P. (1981) *Guignardia bidwellii*. *CMI Descriptions of Pathogenic Fungi and Bacteria*, 710.

Sivanesan A., Waller J., Mordue J. (1974) *Venturia inaequalis*. *CMI Descriptions of Pathogenic Fungi and Bacteria*, 401–410.

Sofi K.G., Metzger C., Riemann M., Nick P. (2023) Chitosan triggers Actin remodelling and activation of defence genes that is repressed by calcium influx in grapevine cells. *Plant Science*, **326**, 111527.

Taraschewski H. (2006) Hosts and parasites as aliens. *Journal of Helminthology*, **80**, 99–128.

Ullrich C.I., Kleespies R.G., Enders M., Koch E. (2009) Biology of the black rot pathogen, *Guignardia bidwellii*, its development in susceptible leaves of grapevine *Vitis vinifera*. *Journal für Kulturpflanzen*, **61**, 82–90.

Valsangiacomo C., Gessler C. (1992) Purification and characterization of an exo-polygalacturonase produced by *Venturia inaequalis*, the causal agent of apple scab. *Physiological and Molecular Plant Pathology*, **40**, 63–77.

Wikee S., Lombard L., Nakashima C., Motohashi K., Chukeatirote E., Cheewangkoon R., McKenzie E.H., Hyde K.D., Crous P.W. (2013) A phylogenetic re-evaluation of *Phyllosticta* (Botryosphaeriales). *Studies in Mycology*, **76**, 1–29.